

Supplementary Material for Synthesis of Energy-Bounded Planar Caging Grasps using Persistent Homology

Jeffrey Mahler^{1,*}, Florian T. Pokorny^{1,2,*}, Sherdil Niyaz¹, Ken Goldberg¹

¹AUTOLAB and Berkeley Artificial Intelligence Research Laboratory
Dept. of IEOR and EECS, University of California, Berkeley, USA
{jmahler, sniyaz, goldberg}@berkeley.edu

² CAS/CVAP, KTH Royal Institute of Technology, Sweden
fpokorny@kth.se

This document contains select proofs for Theorems and additional experimental data for the paper “Synthesis of Energy-Bounded Planar Caging Grasps using Persistent Homology,” currently under review for the 12th International Workshop on the Algorithmic Foundations of Robotics.

1 Correctness of EBCS-2D

Energy-Bounded-Cage-Synthesis-2D (EBCS-2D), detailed in Algorithm 1, synthesizes energy-bounded cages of a polygonal object \mathcal{O} by a rigid configuration of polygonal obstacles \mathcal{G} with respect to an energy function $U : SE(2) \times SE(2) \rightarrow \mathbb{R}$. We require that the energy function U can be derived from a univariate potential function $P(\mathbf{q}) : SE(2) \rightarrow \mathbb{R}$, $U(\mathbf{q}_i, \mathbf{q}_j) = P(\mathbf{q}_i) - P(\mathbf{q}_j)$. We refer to poses as $\mathbf{q} = (x, y, z) \in SE(2)$. See [3] or the main text for further definitions.

Theorem 1 (Correctness of EBCS-2D). *Assume the object is specified as a compact polygon $\mathcal{O} \subset \mathbb{R}^2$ and the obstacles are defined a rigid configuration of a set of k polygons $\mathcal{G} = \mathcal{P}_1 \cup \dots \cup \mathcal{P}_k \subset \mathbb{R}^2$. Furthermore, assume the energy function $U : SE(2) \times SE(2) \rightarrow \mathbb{R}$ satisfies the following:*

1. $U(\mathbf{q}, \mathbf{q}) = 0$ for all $\mathbf{q} \in SE(2)$.
2. $U(\mathbf{q}_i, \mathbf{q}_j) = P(\mathbf{q}_i) - P(\mathbf{q}_j)$ for all $\mathbf{q} \in SE(2)$ and a potential function $P : SE(2) \rightarrow \mathbb{R}$.
3. $P((x, y, \cdot)) = c$ for some $c \in \mathbb{R}$ (P does not depend on θ)
4. P is convex on the translational component \mathbb{R}^2 .

Let $\hat{\mathcal{Q}} = \{(\hat{\mathbf{q}}_i, \hat{u}_i)\}_{i=1}^N$ be the list of poses returned by EBCS-2D. For each $(\hat{\mathbf{q}}, \hat{u}) \in \hat{\mathcal{Q}}$, $\hat{\mathbf{q}}$ is a \hat{u} -energy bounded cage of \mathcal{O} with respect to U .

Proof. It suffices to show that $(\hat{\mathbf{q}}, \hat{u})$ will only be added to the solution set $\hat{\mathcal{Q}}$ if $\hat{\mathbf{q}}$ is a \hat{u} -energy bounded cage of \mathcal{O} .

Lemma 1. *Let $D(X, R)$ denote the weighted Delaunay triangulation of the pose samples X and penetration depths R (computed on Line 10). Let $A(X, R) \subset D(X, R)$ denote the weighted alpha shape of X and R at $\alpha = 0$ (computed on*

Line 11). Let π be the covering map defined in Section 4 of [3]. Given any $p \in \mathbb{R}$, let $W_p(X, R) = \{\sigma \in D(X, R) \mid f(\sigma) > p\}$ denote the p -potential forbidden subcomplex of X, R , where:

$$f(\sigma) = \begin{cases} \min_{x \in \sigma} P(\pi(x)) & \sigma \in D(X) - A(X) \\ \infty & \sigma \in A(X) \end{cases}$$

For any pose $\mathbf{q} \in SE(2)$ and $u \in \mathbb{R}$, let $p(\mathbf{q}) = u + P(\mathbf{q})$. Then if $\mathbf{q} \in \mathcal{F}$ is in a bounded path component of $\mathcal{C} - \pi(W_{p(\mathbf{q})}(X, R))$, \mathbf{q} is a u -energy bounded cage of \mathcal{O} .

Proof. The p -potential forbidden subcomplex $W_{p(\mathbf{q})}(X, R) \subset V_u(X, R)(\mathbf{q})$ the u -energy forbidden subcomplex of X, R with respect to \mathbf{q} defined in [3]. This is because $\forall \sigma \in W_{p(\mathbf{q})}(X, R)$, either $\sigma \in A(X, R) \rightarrow \sigma \in V_u(X, R)(\mathbf{q})$ or $P(\sigma) > p(\mathbf{q}) \Leftrightarrow P(\mathbf{q}_i) > p(\mathbf{q}) \forall \mathbf{q}_i \in \sigma \Leftrightarrow P(\mathbf{q}_i) - P(\mathbf{q}) = U(\mathbf{q}_i) > u$. Since $V_u(X, R)(\mathbf{q}) \subset \hat{Z}_u(\mathbf{q})$, the lifted u -energy forbidden space with respect to \mathbf{q} defined in [3]. Recall that $\pi(V_u(X, R)(\mathbf{q})) \subset \mathcal{Z}_u$, the u -energy forbidden space and therefore $\mathcal{C} - \pi(W_{p(\mathbf{q})}(X, R)) \supset \mathcal{F}_u(\mathbf{q})$, the u -energy admissible space defined in [3]. Therefore any path in $\mathcal{C} - \pi(W_{p(\mathbf{q})}(X, R))$ can be restricted to $\mathcal{F}_u(\mathbf{q})$ which implies that \mathbf{q} lies in a bounded-path component of $\mathcal{F}_u(\mathbf{q})$. Thus, by definition \mathbf{q} is a u -energy-bounded cage.

Now define the filtration $K(X, P) : \emptyset = K_0 \subset K_1 \subset \dots \subset K_n \subset D(X, R)$ of simplices in $D(X, R)$ with respect to f . Let $\mathcal{I} = \{(i_m, j_m)\}_{m=1}^M$ denote the set of k persistence pairs for $K(X, P)$ such that $\dim(\sigma_{i_m}) = 2$. Then any pair $(i, j) \in \mathcal{I}$ corresponds to the birth and death of a class of the second homology group H_2 , and therefore σ_j lies in a bounded path component $C(K_i, \sigma_j) \subset D(X, R) - K_i$ [1]. This implies that $\pi(\sigma_j)$ lies in a bounded path component of $\pi(D(X, R) - K_i)$ by Theorem 4.1 of [3]. Let $p = P(\sigma_i)$ and $u(\mathbf{q}) = P(\sigma_i) - P(\mathbf{q})$ for any $\mathbf{q} \in C(K_i, \sigma_j) \cap \mathcal{F}$, if such a pose exists. By the definition of the filtration, $K_i = W_p(X, R)$. By Lemma 1 any $\mathbf{q} \in C(K_i, \sigma_j) \cap \mathcal{F}$ is in a bounded path component and is therefore a $u(\mathbf{q})$ -energy-bounded cage of \mathcal{O} . EBCS-2D only adds $\hat{\mathbf{q}}, \hat{u}$ to the solution set for $\hat{u} = P(\sigma_i) - P(\hat{\mathbf{q}})$ (Line 19) if \mathbf{q} is collision free (Line 20) and in the same bounded path component as σ_j (Line 16), and is therefore correct.

2 Derivation of Energy Field for Constant Velocity Quasi-Static Pushing in the Horizontal Plane

Consider a compact polygonal object $\mathcal{O} \subset \mathbb{R}^2$ of mass $m_{\mathcal{O}}$ and a rigid configuration of a set of k polygonal obstacles $\mathcal{G} = \mathcal{P}_1 \cup \dots \cup \mathcal{P}_k \subset \mathbb{R}^2$ of total mass $m_{\mathcal{G}}$. Denote by $\mathbf{q} \in SE(2)$ the pose of \mathcal{O} relative to the reference frame of \mathcal{G} . Assuming quasi-static conditions and a Coloumb friction model, let the object and gripper rest on a horizontal worksurface a coefficient of friction $\mu \in \mathbb{R}$ under gravity, where $g = 9.81m/s^2$ is the acceleration due to gravity. Assume a uniform pressure distribution for both \mathcal{O} and \mathcal{G} and let the center of mass of each be $\mathbf{x}_{\mathcal{O}}$ and $\mathbf{x}_{\mathcal{G}}$ located at the centroid of the respective pressure distributions.

```

1 Input: Polygonal robot gripper  $\mathcal{G}$ , Polygonal object  $\mathcal{O}$ , Potential function  $P$ ,
   Number of pose samples  $s$ , Number of rotations  $R$  for  $SE(2)$  lifting, Energy
   threshold  $u_t$ 
   Result:  $\hat{\mathcal{Q}}$ , set of energy-bounded cages with estimated escape energies
   // Sample poses in collision
2  $\mathcal{Q} = \emptyset, R = \emptyset, \ell = \text{diam}(\mathcal{G}) + \text{diam}(\mathcal{O})$ ;
3  $\mathcal{W} = [-\ell, \ell] \times [-\ell, \ell] \times [0, 2\pi)$ ;
4 for  $i \in \{1, \dots, s\}$  do
5    $\mathbf{q}_i = \text{RejectionSample}(\mathcal{W})$ ;
6    $r_i = \text{LowerBoundPenDepth}(\mathbf{q}_i, \mathcal{O}, \mathcal{G})$ ;
7   if  $r_i > 0$  then
8      $\mathcal{Q} = \mathcal{Q} \cup \{\mathbf{q}_i\}, R = R \cup \{r_i\}$ ;
9   end
10  $X = \{\pi_n^{-1}(\mathbf{q}_i) \mid \mathbf{q}_i \in \mathcal{Q}, n \in \{-N_r, \dots, N_r\}\}$ ;
   // Create alpha shape
11  $D(X, R) = \text{WeightedDelaunayTriangulation}(X, R)$ ;
12  $A(X, R) = \text{WeightedAlphaShape}(D(X, R), \alpha = 0)$ ;
   // Run Persistent Homology
13  $K = \text{Filtration}(D(X, R), A(X, R))$ ;
14  $\Delta = \text{ComputeSecondHomologyPersistencePairs}(K)$ ;
   // Find Energy-Bounded Cages
15 for  $(i, j) \in \Delta$  do
16    $C(K_i, \sigma_j) = \text{PathComponent}(\sigma_j, K_i)$ ;
17   for  $\sigma \in \text{Sorted}(C(K_i, \sigma_j), P)$  do
18      $\mathbf{q} = \text{Centroid}(\sigma)$ ;
19      $u = P(\sigma_i) - P(\mathbf{q})$ ;
20     if  $\text{CollisionFree}(\mathbf{q})$  and  $u > u_t$  then
21        $\hat{\mathcal{Q}} = \hat{\mathcal{Q}} \cup \{(\mathbf{q}, u)\}$ ;
22     end
23   end
24 end
25 return  $\hat{\mathcal{Q}}$ ;

```

Algorithm 1: Energy-Bounded-Cage-Synthesis-2D

Now let \mathcal{G} push along a fixed direction with constant translational velocity of magnitude $\beta \in \mathbb{R}$ in direction $\hat{\mathbf{v}} \in \mathcal{S}^1$ and zero angular velocity. When \mathcal{O} is not in contact with \mathcal{G} , we assume it moves with constant translational velocity $V_O = -\beta\hat{\mathbf{v}}$ relative to \mathcal{G} . When \mathcal{O} is in contact with \mathcal{G} , we assume it moves with constant translational velocity V_O with magnitude $\|V_O\|_2 \leq \beta$ relative to \mathcal{G} . Zero net force must be acting on \mathcal{O} to maintain constant velocity, and therefore the forces due to pushing $f_p = -f_f$, where f_f are the forces due to friction. Thus the motion of \mathcal{O} relative to \mathcal{G} can be described by an applied force $f_p = -\gamma\hat{\mathbf{v}}$ in the reference frame of \mathcal{G} , where the magnitude of forces cannot exceed the maximum force due to friction $\gamma < \mu(m_O + m_G)g$. This translational force may be applied through contact between \mathcal{G} and \mathcal{O} , and therefore f_p can exert a torque τ_p on \mathcal{O} relative to \mathcal{G} such that $\tau_p \leq \rho f_p$, where $\rho \in \mathbb{R}$ is the maximum moment arm of \mathcal{O} [5, 4, 6].

To derive the energy function, consider the amount of energy (mechanical work) that a time-varying external wrench $w_e(t) = (f_e(t), \tau_e(t))$ would have to exert to move \mathcal{O} along a continuous path $\gamma : [0, 1] \rightarrow SE(2)$ from pose \mathbf{q}_i to \mathbf{q}_j (e.g. $\gamma(0) = \mathbf{q}_i, \gamma(1) = \mathbf{q}_j$) with a constant magnitude velocity η under the constant pushing wrench $w_p = (f_p, \tau_p)$ and time-varying wrenches due to friction $w_f(t) = (f_f(t), \tau_f(t))$ [2]:

$$\mathcal{E}(w_e, \gamma) = \int_0^1 w_e(t) \cdot \dot{\gamma}(t) dt$$

By the constant velocity assumption, the kinetic energy of the object does not change. Therefore the net work done on the object over the path γ is zero due to conservation of energy:

$$\begin{aligned} \mathcal{E}(w_e + w_p + w_f, \gamma) &= \int_0^1 (w_e(t) + w_p + w_f(t)) \cdot \dot{\gamma}(t) dt = 0 \\ &\Rightarrow \mathcal{E}(w_e, \gamma) = -\mathcal{E}(w_p + w_f, \gamma) \end{aligned}$$

We can upper bound the amount of work done by the constant pushing wrench w_p and time-dependent frictional wrench w_f using Cauchy-Schwarz:

$$\begin{aligned} \mathcal{E}(w_p + w_f, \gamma) &= \int_0^1 w_p \cdot \dot{\gamma}(t) dt + \int_0^1 w_f(t) \cdot \dot{\gamma}(t) dt \\ &= w_p \cdot \int_0^1 \dot{\gamma}(t) dt + \int_0^1 w_f(t) \cdot \dot{\gamma}(t) dt \\ &\leq \mu(m_O + m_G)g\hat{\mathbf{v}} \cdot (\mathbf{x}_j - \mathbf{x}_i) + \rho\mu(m_O + m_G)g(\theta_j - \theta_i) \\ &\quad + \mu(m_O + m_G)g \int_0^1 \|\dot{\gamma}(t)\|_2 dt \text{ (by Cauchy-Schwarz)} \\ &\leq \mu(m_O + m_G)g\hat{\mathbf{v}} \cdot (\mathbf{x}_j - \mathbf{x}_i) + 2\pi\rho\mu(m_O + m_G)g + \eta\mu(m_O + m_G)g \\ &= \mu(m_O + m_G)g\hat{\mathbf{v}} \cdot (\mathbf{x}_j - \mathbf{x}_i) + \mu(m_O + m_G)g(2\pi\rho + \eta) \end{aligned}$$

And therefore under our assumptions we can lower bound the energy exerted by any external wrenches by:

$$\begin{aligned} U(\mathbf{q}_j, \mathbf{q}_i) &= F_p \hat{\mathbf{v}} \cdot (\mathbf{x}_j - \mathbf{x}_i) - \kappa(\mathcal{O}, \mathcal{G}, \mu) \\ F_p &= -\mu(m_O + m_G)g \\ \kappa(\mathcal{O}, \mathcal{G}, \mu) &= \mu(m_O + m_G)g(2\pi\rho + \eta) \end{aligned}$$

This motivates our use of the linear, univariate potential $P(\mathbf{q}) = F_p \hat{\mathbf{v}} \cdot (\mathbf{x}_j - \mathbf{x}_i)$.

3 Additional Notes on Experiments

3.1 Persistence Diagrams for Real Data

To further illustrate the notion of persistence, we study the persistence diagrams of the second homology group for a single object and the Zymark Zymate gripper in Fig. 1. To generate the diagram we constructed the weighted Delaunay triangulation and α -shape using $s = 200,000$ pose samples and examined the list Δ generated on Line 14 of Algorithm 1. We see that the three energy-bounded cages returned by EBCS-2D correspond to the three most persistent pairs, which appear furthest from the diagonal. Furthermore, our algorithm correctly identifies the large number of candidate configurations with very low persistence.

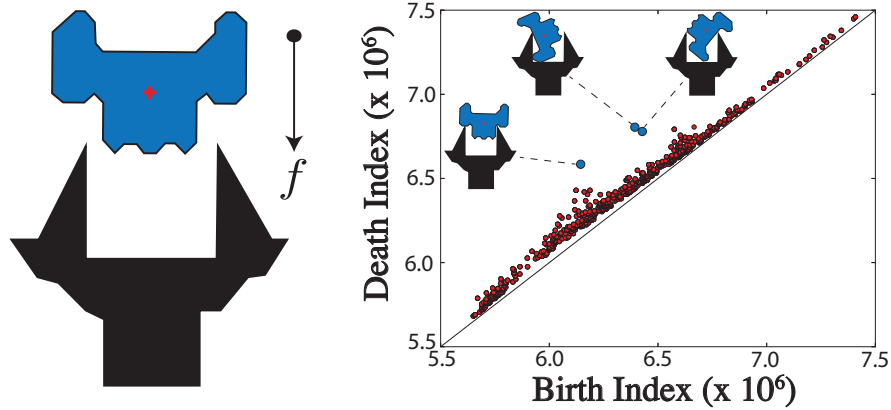


Fig. 1: Persistence diagram for the second homology persistence pairs (corresponding to “voids”) in the filtration K identified during a run of EBCS-2D with $s = 200,000$ pose samples and an energy threshold of $u_t = 0.5$ for a part (blue) and gripper configuration (black) with a vertical push force. The (i, j) coordinate for each point corresponds to the birth and death indices of the voids. Points in red were pruned by our algorithm. The three points in blue were identified by EBCS-2D as energy-bounded cages, and their corresponding workspace configurations are illustrated next to the points.

3.2 Numeric Issues in Implementation

In order for EBCS-2D to be correct, the computed penetration depth r_i for a pose \mathbf{q}_i must not be greater than the true 2D generalized penetration depth, $r_i \leq p(\mathbf{q}_i)$. This can be theoretically achieved using the lower-bound algorithm given by Zhang et al. [8] by taking the maximum of the exact penetration depth between pairs of convex pieces in a convex decomposition of the object and obstacles, where the exact penetration depth can be computed with the Gilbert-Johnson-Keerthi Expanding Polytope Algorithm (GJK-EPA) [7]. However, in practice GJK-EPA computes the exact penetration depth up to some tolerance $\pm\epsilon$. Thus to avoid mis-identifying a configuration as a complete or energy-bounded cage, in practice we use $r_i = \max(\hat{r}_i - \epsilon, 0)$, where \hat{r}_i is the penetration depth computed using the algorithm of Zhang et al. [8]. To avoid further numeric issues related to imprecision in the convex decomposition, computation of the maximum moment arm, or the triangulation, in practice it may be beneficial to additionally multiply the returned penetration depth by some shrinkage factor $0 < \nu < 1$, $r_i = \nu \max(\hat{r}_i - \epsilon, 0)$.

References

1. H. Edelsbrunner and J. Harer, *Computational topology: an introduction*. American Mathematical Soc., 2010.
2. D. C. Giancoli, *Physics: principles with applications*. Pearson Education, 2005.
3. J. Mahler, F. T. Pokorny, A. F. van der Stappen, and K. Goldberg, “Energy-bounded caging: Formal definition and 2d lower bound algorithm based on weighted alpha shapes,” in *IEEE Robotics & Automation Letters*. IEEE, 2016.
4. M. T. Mason, “Mechanics and planning of manipulator pushing operations,” *The International Journal of Robotics Research*, vol. 5, no. 3, pp. 53–71, 1986.
5. —, *Mechanics of Robotic Manipulation*. Cambridge, MA, USA: MIT Press, 2001.
6. M. A. Peshkin and A. C. Sanderson, “The motion of a pushed, sliding workpiece,” *IEEE Journal on Robotics and Automation*, vol. 4, no. 6, pp. 569–598, 1988.
7. G. Van Den Bergen, “Proximity queries and penetration depth computation on 3d game objects,” in *Game developers conference*, vol. 170, 2001.
8. L. Zhang, Y. J. Kim, and D. Manocha, “Efficient cell labelling and path non-existence computation using c-obstacle query,” *The International Journal of Robotics Research*, vol. 27, no. 11-12, pp. 1246–1257, 2008.